Superconductivities and structural properties of ternary Ti–Zr–Ta alloys*

Wang Zhi-Wei(王秩伟), Jia Li(贾 丽), Yang Huai-Xin(杨槐馨), Tian Huan-Fang(田焕芳), Shi Hong-Long(施洪龙), Wang Zhen(王 臻), and Li Jian-Qi(李建奇)†

Beijing National Laboratory for Condensed Matter Physics, Institute of Physics, Chinese Academy of Sciences, Beijing 100190, *China*

(Received 15 June 2011; revised manuscript received 9 August 2011)

Superconductivities and structural properties of Ti–Zr–Ta ternary alloys are extensively investigated. The TiZrTa sample has a cubic structure (β-phase) and shows a sharp superconducting transition at a critical temperature (T_c) of about 7.3 K. In addition, two series of Ti–Zr–Ta alloys, with nominal compositions of $Ti_{65-x}Zr_{35}Ta_x$ and $Ti_xZr_{65-x}Ta_{35}$ respectively, are prepared, and their superconductivities and crystal structures change regularly with the chemical composition. Our experimental study also indicates that the annealing processing of this kind of material can cause the transition temperature to increase and the highest T_c is observed to be about 8.3 K in annealed samples.

Keywords: Ti–Zr–Ta alloys, superconductivity, crystal structure, X-ray diffraction

PACS: 74.70.Dd, 74.25.–q, 74.62.–c **DOI:** 10.1088/1674-1056/20/11/117402

1. Introduction

The superconductivities and the high critical fields (H_c) for the Nb-based binary solution alloys, such as Ti–Nb or Zr–Nb, have been of technological and academic interest for decades, as this kind of alloy generally has excellent mechanical properties and good fabricability and is often used for fabricating conductors for large superconducting devices.[1−4] Meanwhile, the superconductivities in the Ta-based binary alloys such as Ti–Ta, Ta–Sn and Ta–C have also been studied for many years [5−7]. From the structural point of view, these alloys mostly exhibit two stable structures, i.e. the β phase with body-centred-cubic (bcc) structure and the α phase with hexagonal closed-pack (hcp) structure. Occasionally, certain metastable phases can also be observed in these materials during heating treatment or mechanical processing. In previous publications, superconductivities, crystal structures and the high-pressure behaviours of binary (Nb, Ta or Ti)-based alloys have been extensively studied.[8−10]. For instance, Bashkin *et al.*[11] reported that the structural transition from the α phase to the β phase in TiZr alloy relates to an increase of the superconducting T_c under a high pressure. In addition, our previous studies of the superconductivities in Ti–Zr–Nb ternary alloys in correlation with microstructure features have revealed that the Ti–Zr–Nb system has a cubic structure (the β-phase) and shows up the superconductivity for Nb in a large range; and the superstructure phase in general coexists with the cubic β-phase, thereby yielding two superconducting transitions.[12] In the present paper, we report on the superconductivities observed in Ti–Zr–Ta ternary materials, and we also discuss the effects of annealing on superconducting and structural property.

2. Experimental details

All Ti–Zr–Ta alloys used in the present study were prepared by arc-melting high-purity titanium, zirconium, and tantalum (all better than 99.9%) in melting furnace with a non-consumable tungsten electrode and a water-cooled copper hearth under an ultra-pure argon atmosphere. The ingot alloys were remelted a few times for homogeneity in composition and microstructure, and then suction-cast into 1 mm thickness pieces for further study. For annealing process, samples were sealed into an evacuated ($\approx 10^{-5}$ Pa) quartz tube and slowly heated to 800 °C and stayed at this temperature for 72 h. The X-ray diffraction (XRD) measurements were performed on an X-ray powder diffrac-

*Project supported by the National Natural Science Foundation of China (Grant Nos. 10874227, 11074292, and 10904166).
†Corresponding author. E-mail: ljq@aphy.iphy.ac.cn
© 2011 Chinese Physical Society and IOP Publishing Ltd

tometer with Cu$K\alpha$ radiation at 2θ from 20° to 90°. The chemical composition was checked by using of energy dispersive X-ray (EDX) semiquantitative analysis on a Hitachi S-4800 SEM. The temperature dependence of electrical resistivity $\rho(T)$ was measured by a standard four-point probe method, and the effect of applied magnetic field on ρ was measured using a quantum design physical property measurement system. The temperature dependence of alternating current (AC) magnetic susceptibility $\chi(T)$ was measured by using quantum design superconducting quantum interference device (SQUID) magnetometer at a magnetic field of 1 Oe (1 Oe=79.5775 A/m) with the frequency of 333 Hz.

3. Results and discussion

Figure 1(a) shows a typical XRD pattern of the as-cast TiZrTa sample, in which all the diffraction peaks could be well indexed to the cubic structure with the lattice parameter of $a = 3.388(2)$ Å and a space group of *Im-3m*. No impurity peak such as TiTa or ZrTa was detected in our measurements. The inset of Fig. 1(a) illustrates a structural model of TiZrTa. The EDX analysis was used to check the chemical composition of a typical sample, and the average ratio of the elements is estimated to be Ti:Zr:Ta=31.7:34.7:33.6, which is almost consistent with the nominal 1:1:1 stoichiometry within the experimental error. The temperature dependence of resistivity for TiZrTa sample at zero applied magnetic field is shown in Fig. 1(b), indicating a clear superconducting transition with a critical temperature (T_c) of about 7.3 K. We herein define T_c as the onset temperature of the downturn in the $\rho(T)$ curve. It is also noted that this superconductor above T_c shows a metallic behaviour in the normal state and the superconducting transition is sharp with a transition width of less than 0.5 K, indicating the fine homogeneity of the sample. Figure 1(c) shows the temperature dependence of AC magnetic susceptibility $\chi(T)$ for this sample. Superconducting transitions in both real part (χ') and imaginary part (χ'') of the susceptibility data is clearly recognizable at about 7 K in consistence with the resistivity measurements as shown in Fig. 1(b).

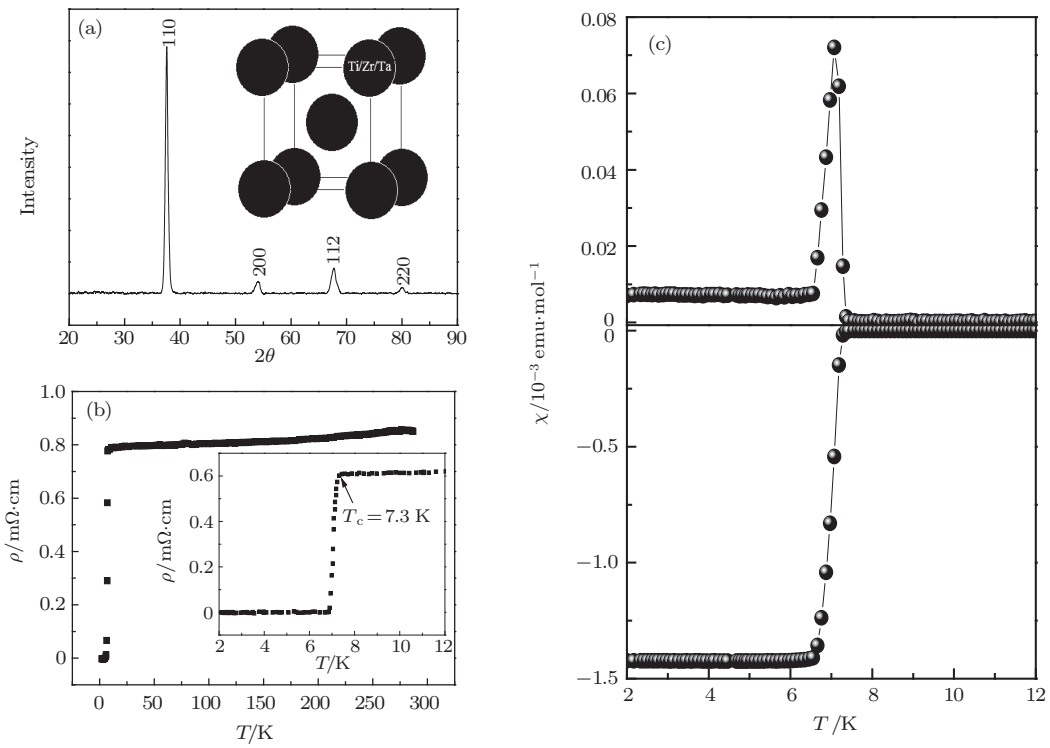


Fig. 1. (a) XRD patterns of as-cast TiZrTa sample, showing the cubic structure with a lattice parameter of about 3.388(2) Å, where the inset illustrates the atomic structure of this sample. (b) Temperature dependences of resistivity and (c) AC magnetic susceptibility for TiZrTa sample, clearly exhibiting superconducting transition with T_c being about 7.3 K (1 emu=10^{-3} A·m^2), and the inset in panel (b) shows resistivity behaviour through superconducting transition and the critical transitions (T_c) is indicated by an arrow.

In order to obtain the Ti–Zr–Ta samples with higher T_c, we examine numerous samples with different compositions, and two series of samples with nominal compositions of $Ti_{65-x}Zr_{35}Ta_x$ (x = 10, 20, 25, 30, 35, 40, 45, 50, 55, 60), and $Ti_xZr_{65-x}Ta_{35}$ (x = 10, 20, 25, 30, 35, 40, 50) alloys were selected to be discussed in this paper. Figure 2 shows the XRD patterns of $Ti_{65-x}Zr_{35}Ta_x$, which demonstrate that each of all the samples has a cubic structure and no impurity phase appears. It is known that each of binary Ti–Zr alloys often has a hexagonal structure. However, our experimental results suggest that the Ta substitution for Ti is conducible to the stability of the cubic β-phase, and a similar phenomenon was also observed in the ternary Ti–Zr–Nb alloy in which Nb atoms play a key role as the stablizer of the cubic β-phase in our previous study.[12] In addition, it is clear that the diffraction peaks shift toward high diffraction angle (2θ) with the increase of Ta content, demonstrating that the lattice parameters become smaller. It is estimated that the lattice parameter a decreases visibly from 3.385(8) Å for $Ti_{55}Zr_{35}Ta_{10}$ to 3.352(4) Å for $Ti_5Zr_{35}Ta_{60}$ with the increase of Ta content, which demonstrates that the substitution of Ta for Ti can not only yield the variation of crystal symmetry but also lead to a remarkable change in lattice constant.

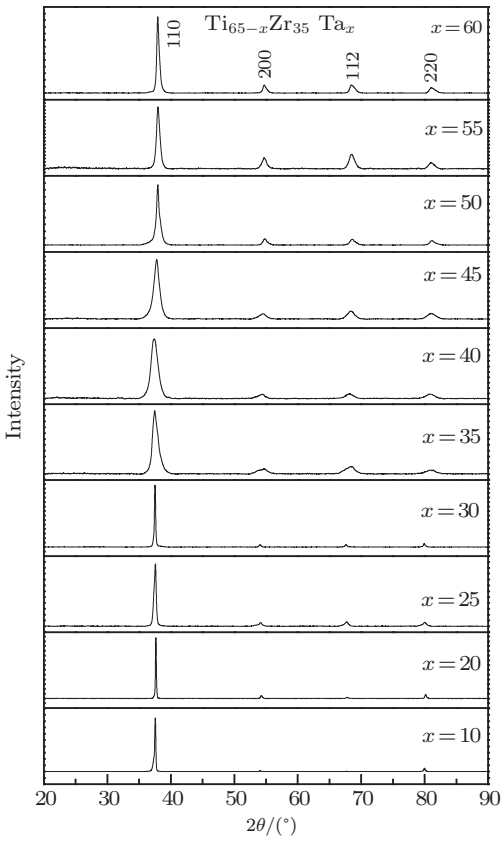


Fig. 2. XRD patterns of $Ti_{65-x}Zr_{35}Ta_x$ samples with x ranging from 10 to 60, demonstrating clearly that the diffraction peaks shift regularly with the increase of x.

Figure 3(a) shows the temperature dependences of resistivity $Ti_{65-x}Zr_{35}Ta_x$ samples with x = 10, 20, 25, 40 and 60. It is recognizable that all samples show superconducting transitions with the values of critical temperature T_c ranging from 3.6 K to 8.3 K. The superconducting transitions in general are very sharp with the transition widths less than 0.5 K for most samples. Figure 3(b) clearly illustrates that the T_c in each of these samples increases gradually with the rise of Ta content. Figure 3(c) shows the resistivities versus temperature for sample $Ti_{30}Zr_{35}Ta_{35}$ under the applied magnetic field H = 1, 3, 5, 7, and 9 T, illustrating that the T_c decreases from 7.5 K to 3.5 K with the increase of magnetic field. Figure 3(d) illustrates the temperature dependence of upper critical field $H_{c2}(T)$. According to the weak-coupling Bardeen–Cooper–Schrieffer (BCS) theory, the upper critical field at $T = 0$ K can be determined by the Werthamer–Helfand–Hohenberg (WHH) equation[13] to be $H_{c2}(0) = -0.693[(dH_{c2}/dT)]_{T_c}T_c$. From Fig. 3(d), one can obtain that $-dH_{c2}/dT = 2.38\ T/\mathrm{K}$ and $T_c = 7.5$ K, then the $H_{c2}(0)$ can be estimated to be about 12.4 T. This value is slightly higher than that of TiZrNb ternary superconductor.[14] The temperature dependences of AC magnetic susceptibility $\chi(T)$, for samples, of x = 30, 35, 45 are presented in Fig. 3(e), showing clearly superconducting transitions in both real (χ') and imaginary parts (χ''). Note that in the imaginary part of AC susceptibility for some of the studied samples there appear two peaks. This phenomenon is similar to that observed in our previous study of Ti–Zr–Nb system. In Ti–Zr–Nb system, the two peaks indicate two superconducting transitions, which relates to the specific superstructure property. Therefore, here the two peaks may also relate to a specific structure, which needs further study.

In order to study the effect of Ti (Zr) content on the superconductivity and structure property in Ti–Zr–Ta system, we also study another series of samples with a fixed Ta content, i.e., $Ti_xZr_{65-x}Ta_{35}$. Figure 4 shows the XRD patterns of as-cast samples. It is demonstrated that the crystal structure changes with the increase of Ti content. Samples with x values ranging from 10 to 25 show certain complex structural features due to the coexistence of a cubic structure (the β phase) and an orthorhombic structure (the

α'' phase) as indicated by a rectangle in Fig. 4. Samples with x values ranging from 30 to 50 each has a cubic structure and no peaks of other phases are observed. Moreover, the diffraction peaks of the β phase each shifts progressively toward larger diffraction angle with the increase of Ti content, which is clearly illustrated in Fig. 4, where the remarkable changes of the lattice parameters for samples with different amounts of Ti content can be clearly seen. Each sample with low Ti content often has a mixture structure. The values of lattice parameter a for β phase are estimated to be about 3.459(8) Å and 3.367(5) Å for $x = 10$ and 25, respectively. Each sample with high Ti content has a cubic structure, the lattice parameter a decreases from 3.347(8) Å for $x = 30$ to 3.327(3) Å for $x = 50$. This change is caused mainly by the difference in atomic size between Ti ($\sim$ 2.00 Å) and Zr ($\sim$ 2.16 Å).

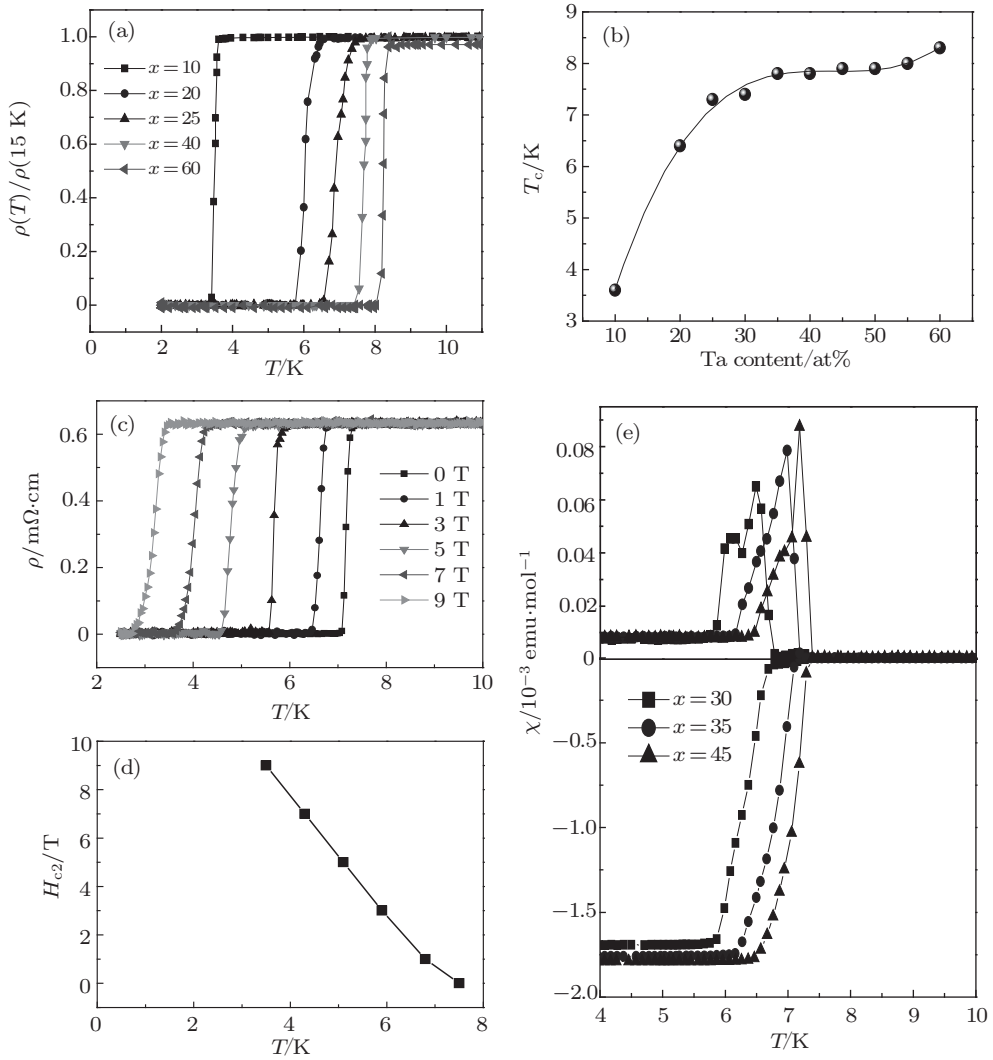


Fig. 3. (a) Temperature dependences of resistivity for typical $Ti_{65-x}Zr_{35}Ta_x$ samples with x = 10, 20, 25, 40 and 60, illustrating the variations of T_c from 3.5 K to 8.3 K. (b) The relationship between the T_c and Ta content of $Ti_{65-x}Zr_{35}Ta_x$ samples. (c) $\rho(T)$ curves measured under applied magnetic field H = 0, 1, 3, 5, 7, and 9 T for $Ti_{30}Zr_{35}Ta_{35}$ alloy. (d) Temperature dependences of upper critical field $H_{c2}(T)$ for $Ti_{30}Zr_{35}Ta_{35}$. (e) AC magnetic susceptibilities for samples with x = 30, 35 and 45.

Figure 5(a) shows the temperature dependences of resisitivity of typical $Ti_xZr_{65-x}Ta_{35}$ samples with x = 10, 30, 35, and 50. All samples show clear superconducting transitions but the transition temperatures change continuously with the Ti concentration, and the highest T_c is 7.8 K for the sample of $x = 30$. Figure 5(b) clearly exhibits the T_c in this series of sample varies with the rise of Ti content. The superconducting transitions, similar to those in $Ti_{65-x}Zr_{35}Ta_x$ samples, are very sharp, the transition width is less than 0.5 K for most samples.

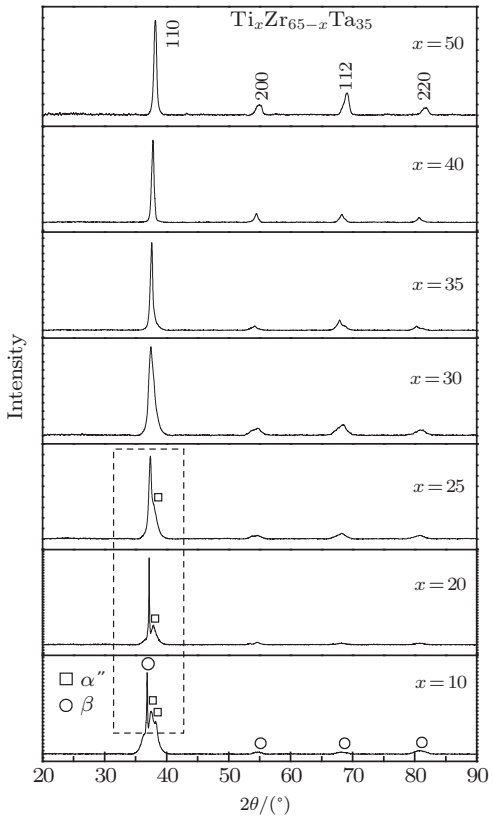


Fig. 4. XRD patterns of $Ti_xZr_{65-x}Ta_{35}$ samples with x values ranging from 10 to 50, showing that samples with $x > 30$ each has a cubic structure and samples with $x < 25$ often exhibit complex structural features due to the coexistence of cubic and rthorhombic structures.

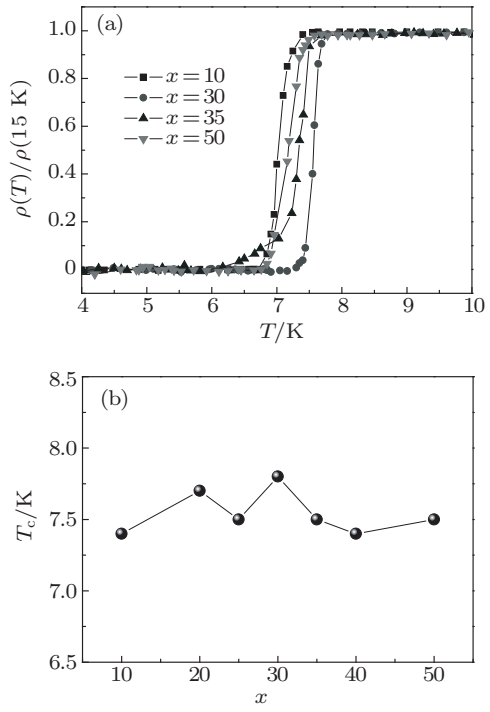


Fig. 5. (a) Temperature dependences of resistivity for $Ti_xZr_{65-x}Ta_{35}$ materials with x = 10, 30, 35 and 50. (b) The relationships between the T_c and Ti content for $Ti_xZr_{65-x}Ta_{35}$ materials.

In order to further enhance the T_c in the present system, we perform experiments on some samples by different annealing processes; the results demonstrate that annealing process can increase the value of T_c in a certain case. Figure 6(a) shows the temperature dependences of resistivity of samples of TiZrTa and $Ti_{35}Zr_{35}Ta_{30}$ annealed at 800 °C under a high vacuum for 72 h. It is evident that the T_c increases from 7.3 K for as-cast TiZrTa sample to 8.3 K for annealed one; and for $Ti_{35}Zr_{35}Ta_{30}$ sample, it increases from 7.4 K to 7.9 K as seen from the $\rho(T)$ curves. It also noted that the superconducting transitions are more sharp with the transition widths less than 0.2 K. This fact suggests that the annealed samples should have a much more homogenous microstructure than the as-cast sample. Figure 6(b) shows the temperature dependences of AC magnetic susceptibility for two typical samples. The T_c value is higher than that of as-cast sample as shown in Figs. 1(c) and 3(e), which is consistent with the results from $\rho(T)$ curves.

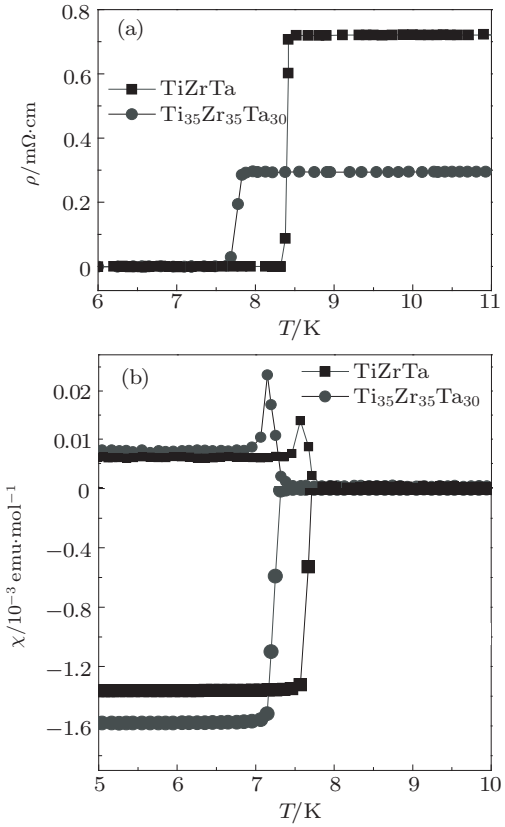


Fig. 6. Temperature dependences of (a) resistivity and (b) AC magnetic susceptibility for annealed TiZrTa and $Ti_{35}Zr_{35}Ta_{30}$ samples, showing that the values of critical temperature T_c are respectively enhanced to 8.3 K and 7.9 K in the annealed samples.

4. Conclusions

A variety of Ti–Zr–Ta ternary alloys are synthesized by arc-melting method, and the superconductivities and the structural properties are extensively discussed in the cases of different chemical compositions. TiZrTa sample has a cubic structure with lattice parameter $a = 3.388(2)$ Å and exhibits a superconducting transition at $T_c = 7.3$ K. $Ti_{65-x}Zr_{35}Ta_x$ and $Ti_xZr_{65-x}Ta_{35}$ alloys show clearly superconductivity changing continuously with chemical composition. In addition, annealing processing of this kind of material can lead to the notable enhancement of superconductivity in certain samples. All samples show sharp superconducting transitions and the highest critical temperature T_c is observed to be 8.3 K. The $H_{c2}(0)$ is estimated to be about 12.4 T for sample $Ti_{30}Zr_{35}Ta_{35}$.

References

[1] Neuringer L J and Shapira Y 1966 *Phys. Rev.* **148** 231

[2] Berlincourt T G and Hake R R 1963 *Phys. Rev.* **131** 140

[3] Vonsovsky S V, Izyumov Y A and Kurmaev E Z 1982 *Superconductivity of Transition Metals Their Alloy and Compounds* (translated by Brandt E H and Zavarnitsyn A P) (New York: Springer) p. 231

[4] Poole Jr C P, Farach H A, Creswick R J and Prozorov R 2007 *Superconductivity* (2 edn) (Amsterdam: Academic Press of Elsevier) p. 71

[5] Savitskii E M, Efimov Y V and Kozlova N D 1971 *Izv. Akad. Nauk SSSR, Met* **4** 214

[6] Corsan J M and Cook A J 1969 *Phys. Lett.* A **28** 500

[7] Narlikar A V and Dew-Hughes D 1967 *J. Mater. Sci.* **2** 496

[8] Neuringer L J and Shapira Y 1966 *Phys. Rev. Lett.* **17** 81

[9] Rapp O 1971 *Solid State Commun.* **9** 1

[10] Mclnturff A D 1969 *J. Appl. Phys.* **40** 2080

[11] Bashkin I O, Fedotov V K, Nefedova M V, Tissen V G, Ponyatovsky E G, Schiwek A and Holzapfel W B 2003 *Phys. Rev.* B **68** 054401

[12] Wang Z W, Li Y, Ma C, Wang Z, Yang H X, Tian H F, Shi H L, Jia L, Zhang F and Li J Q (unpublished)

[13] Werthamer N R, Helfand E and Hohenberg P C 1966 *Phys. Rev.* **147** 295

[14] Ralls K M, Rose R M and Wulff J 1980 *J. Appl. Phys.* **51** 3316